EVALUATION OF CENTRIFUGAL COMPRESSOR STABILITY MARGIN AND INVESTIGATION OF ANTISWIRL MECHANISM

by
Jiming Li
Development Engineer
Pranabesh De Choudhury
Senior Consulting Engineer
and
Frank Kushner
Senior Consulting Engineer
Elliott Company
Jeannette, Pennsylvania

Jiming Li is a Development Engineer of advanced technology at Elliott Company, in Jeannette, Pennsylvania. In his present assignment, he has had responsibility for rotordynamics, torsional vibration analysis, vibration troubleshooting, development and application of advanced damper seals and bearings in turbomachinery since 1998. Dr. Li also has previous experience of more than seven years with rotordynamic tests and computer program development, vi-bration monitoring, and analysis at Zhengzhou Institute of Technology. He has written several technical papers for ASME journals and is a member of ASME.

Dr. Li received a BSME degree (1982) from Zhengzhou Institute of Technology, and obtained MSME (1995) and Ph.D. (1999) degrees (Mechanical Engineering) from Texas A&M University.

Pranabesh De Choudhury has worked for Elliott Company, in Jeannette, Pennsylvania, for the past 32 years in the area of rotor bearing system dynamics. In his current position as Senior Consulting Engineer, his responsibilities include rotor-bearing dynamics, bearing design and analysis, torsional dynamics, blade vibration analysis, and troubleshooting field vibration problems.

Dr. De Choudhury obtained a BSME degree (1963) from Jadavpur University, an MSME degree from Bucknell University, and a Ph.D. degree (Mechanical Engineering, 1971) from the University of Virginia. He has authored and coauthored 24 technical papers and has been awarded a patent. He is a registered Professional Engineer in the State of Pennsylvania and is a member of ASME and STLE.

Frank Kushner is a Senior Consulting Engineer for dynamics and acoustics testing at Elliott Company, in Jeannette, Pennsylvania. He has 34 years' experience with industrial turbomachinery, and four years' previous experience with the combustion section development group at Pratt and Whitney Aircraft. He is a previous author for the Ninth, Twenty-Fifth, Twenty-Ninth, and Thirty-First Turbomachinery Symposia, as well as for ASME.

Mr. Kushner obtained a BSME degree (1965) from Indiana Institute of Technology, and an MSME degree (1968) from Rensselaer Polytechnic Institute. He is a registered Professional Engineer in the State of Pennsylvania and a member of ASME and the Vibration Institute. Mr. Kushner holds patents for a blade damping mechanism and also for a method to prevent one-cell rotating stall in centrifugal compressors.

ABSTRACT

Stringent stability screening criteria by the American Petroleum Institute (API) result in higher level rotor stability analyses to be performed on more intermediate-pressure compressor rotors and in more detail. These high-level stability analyses include predictions of impeller and seal rotordynamic forces and even extra effort on design and analysis of special damping devices as a backup, such as damper bearings and seals. Several moderate-pressure compressors were selected here to discuss the use of stability screening diagrams and the proposed API screening criteria. These compressors are operating successfully with or without a deswirl mechanism. However, most of them fail to pass the proposed new API screening. Furthermore, rotor aerodynamic logarithmic-decrements (log-decrements or log-dec) were predicted by implementing equivalent aerodynamic destabilizing forces that were calculated using Wachel's equation, the API proposed equation, and the original equipment manufacturer's (OEMs) empirical method, respectively. In practice, shunt injection and swirl-brakes are standard tools to enhance rotor stability if the predicted log-decrement is relatively low. When adopted with balance pistons or center seals, the swirl brakes are typically installed behind the impeller and outside the labyrinth seal. However, the deswirl effect of the swirl brake is sometimes limited due to its location away from the entrance of the balance piston or center labyrinth seal. Meanwhile, the implantation of the swirl brake would change the flow pattern behind the final stage impeller backwall. A unique antiswirl brake device was developed to integrate with typical labyrinth seals for improving high-performance compressor stability. The effectiveness of the antiswirl brake mechanism was experimentally investigated when used with the labyrinth seals on a rotating test rig. The gas flow circumferential velocity was measured at the swirl-brake upstream and downstream locations. Test results show the labyrinth seal was converted into a damping device by reducing the preswirl velocity to zero or even negative.

INTRODUCTION

In order to assure that the design of high-performance turbomachinery is acceptable from a rotordynamic point of view, numerous analytical and experimental programs have been conducted to improve the design and the rotordynamic models of the rotating machines. As a critical but delicate part in rotating machines, journal bearings were intensively studied first because the hydrodynamic instability was a long-term unresolved problem before the 1970s. Today, traditional hydrodynamic instability problems in high-speed turbomachinery, such as oil whip, have been fewer with the applications of tilting-pad journal bearings, which have inherently rotordynamic stable characteristics since the bearing cross-coupling stiffness is minimized or even eliminated completely. Oil seals are causes of rotor unstable vibration problems if used improperly. This type of instability vibration only happens on some old compressors having oil seals. Most new compressors are fitted with main dry gas seals, and more and more old compressors have been retrofitted with the dry gas seal to replace the original oil seal. However, chasing a higher unit efficiency results in a more flexible rotor with a higher power density. Load-dependent rotor instability cases are still not uncommon in high-performance centrifugal compressors.

Extensive experimental investigations and field troubleshooting experiences have confirmed the cross-coupling force generated by labyrinth seals to be the major mechanism of inducing a load-dependent instability vibration. So far the OEM and users of turbomachinery are feeling more and more confident in predicting a potential instability problem, as well as identifying and correcting a rotor instability vibration onsite. Much effort has been made through API publications recently to clarify what is the minimum analytical work to be done to ensure a rotordynamic acceptable compressor and protect the customer's interest. Based on the new API standards, a complicated rotordynamic analysis (level-II) has to be performed if any compressor design fails to pass level-I (screening). Obviously, the rotordynamic force coefficients of the labyrinth seals are essential and critical for conducting a level-II rotordynamic stability analysis. Unfortunately, most seal programs are still not validated in suitable operating conditions compared to actual circumstances in which the labyrinth seals are applied. Besides the inherent drawbacks in the seal models, large uncertainties in input data prepared for the computer codes also affect the prediction of labyrinth seal coefficients significantly. For example, both test and prediction have demonstrated that the gas preswirl velocity at the labyrinth seal entrance is one of the most important parameters to determine the seal cross-coupling stiffness. However, to predict the rotordynamic force coefficients of the labyrinth seals, the value of the gas preswirl velocity used in programs has to be assumed by the code users based on different computer programs and individual experience. Conservative assumptions may be applied typically in seal force calculation for safety reasons.

The OEM and users of compressors have known that one of the most effective corrections is to reduce the cross-coupling stiffness of the major labyrinth seals, such as the center seal or the balance piston seal, whenever load-dependent instability becomes a concern in design stages or during field operation. Without doubt, for high-pressure compressors a full stability examination is necessary including bearings and seals, using empirical or standard methods recommended by API. A clear trend is that high-level rotor stability analyses have to be performed on more and more intermediate-pressure compressors based on the new API stability screening requirements. To perform these high-level stability analyses, it would be required to predict labyrinth seal forces accurately and even put extra effort on design and analysis of special damping devices as a backup. Several intermediate-pressure compressors were selected here to discuss using stability screening diagrams and the new API screening criteria. These compressors are operating successfully with or without a deswirl mechanism. However, most of them fail to pass the level-I screening. A unique swirl-brake device was tested and reported in this paper to enhance the rotor stability. The new brake is integrated into typical labyrinth seals to maximize the antiswirl effect of the device without any change in the internal flow pattern inside the rotating machines. The effectiveness of the new antiswirl-brake mechanism was experimentally investigated when used with the labyrinth seals in a rotating test rig.

LABYRINTH SEALS AND THEIR EFFECT ON ROTORDYNAMICS

Widely used as balance drum, interstage, and impeller eye seals to restrict the leakage flows through rotor-stator clearances from a high-pressure region to a low-pressure region, labyrinth seals have been confirmed to be a major source of destabilizing forces resulting in rotordynamic instability problems (Greathead and Bostow, 1976; Doyle, 1980). Labyrinth seal forces are functions of the fluid properties, operating conditions, and geometric configuration. For small amplitudes of rotor motion (X, Y) about an equilibrium position, these forces, $(F_i)_{i=X,Y}$, are typically represented as linearized stiffness, $(K_{i,j})_{i,j=X,Y}$, and damping, $(C_{i,j})_{i,j=X,Y}$, force coefficients (Childs, 1993).

$$\begin{bmatrix} F_X \\ F_Y \end{bmatrix} = \begin{bmatrix} K_{XX} & K_{XY} \\ K_{YX} & K_{YY} \end{bmatrix} \begin{bmatrix} X \\ Y \end{bmatrix} + \begin{bmatrix} C_{XX} & C_{XY} \\ C_{YX} & C_{YY} \end{bmatrix} \begin{bmatrix} \dot{X} \\ \dot{Y} \end{bmatrix} \tag{1}$$

Theoretical analyses based on bulk-flow or CFD models can give all eight rotordynamic coefficients above. For a centered labyrinth seal, it assumes that the direct stiffness and damping coefficients are symmetric ($K_{xx} = K_{yy}$, $C_{xx} = C_{yy}$), and the cross-coupled stiffness and damping coefficients are skew-symmetric ($K_{xy} = -K_{yx}$, $C_{xy} = -C_{yx}$). Accurate seal force coefficients are necessary to predict correctly the critical speeds and dynamic stability of the rotor/bearing/seal systems. Benckert and Wachter (1980) presented an early comprehensive experimental investigation of the flow-induced forces in gas labyrinth seals. Their tests demonstrated that the cross-coupled stiffness coefficient, K_{xy}, depends strongly on the gas preswirl velocity at the labyrinth seal entrance. Childs and Scharrer (1986 and 1988) performed extensive experiments to measure the rotordynamic coefficients of both teeth-on-rotor (TOR) and teeth-on-stator (TOS) labyrinth seals. The seal stiffness and damping coefficients were identified from the measured mechanical impedances. Measurements showed that the seal direct damping, C_{xx}, is positive, but small, and direct force coefficients (K_{xx}, C_{xx}) are sensitive to the supply pressure, though insensitive to the rotor speed and inlet preswirl.

The influence of labyrinth seal forces on rotor vibration can be illustrated in Figure 1, in which a running rotor is whirling along its motion orbit at a whirling frequency Ω. The rotor speed is ω. The seal force applied on the rotor can be expressed in radial and tangential components (F_r, F_t). In practice, it is not uncommon to neglect the cross-coupled damping coefficients (C_{xy}, C_{yx}) for gas labyrinth seals. In the radial direction, the system stiffness would be affected more or less by the seal direct stiffness K_{xx}, which is relatively small compared to bearing stiffness and shaft stiffness. In the tangential direction, a positive force, F_t, would energize the rotor whirling in the shaft rotating direction. Another alternative to illustrate the dynamic characteristics of the labyrinth seal is to define the seal effective stiffness and damping coefficients.

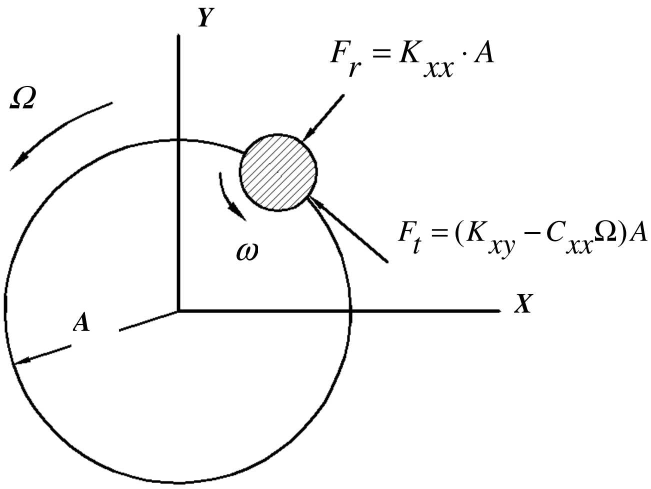

Figure 1. Labyrinth Seal Forces Applied on Whirling Rotor.

$$K_{ef} = K_{xx}$$
$$C_{ef} = C_{xx}\left(1 - \frac{K_{xy}}{\Omega\, C_{xx}}\right) = C_{xx}\left(1 - \frac{K_{xy}}{\omega C_{xx}}\left(\frac{\omega}{\Omega}\right)\right) \tag{2}$$

It is clear in Equation (2) that the seal effective damping, C_{ef}, is not only dependent on the term ($K_{xy}/\omega C_{xx}$), but also the rotor whirling ratio (ω/Ω). Here ($K_{xy}/\omega C_{xx}$) is the ratio of the promoting force ($K_{xy}A$) to the damping force ($\omega C_{xx}A$) for a rotor vibration, and (ω/Ω) is the ratio of angular velocities between rotor running and rotor whirling. Any factors, which promote the seal cross-coupled stiffness and the whirling ratio, would reduce the seal effective damping. At a given rotor speed, Equation (2) also indicates that the seal effective damping is less for subsynchronous rotor vibration compared to synchronous rotor vibration. Therefore, an instability vibration often occurs at the first forward mode of a flexible rotor. It should be pointed out that the positive direct damping C_{xx} of the labyrinth seal is small, but it is critical to keep the rotor in a stable region when the machine is designed with a very narrow stable margin. From a rotordynamics point of view, large positive direct damping coefficients C_{xx} and small positive or even negative cross-coupled stiffness coefficients K_{xy} are desired to suppress rotor vibration and to improve rotor stability in high-performance turbomachinery.

The magnitude of a damping force is proportional to the vibration amplitude of the object on which the damping device acts. Figure 2 shows the typical mode shape of a back-to-back compressor rotor whirling at its first natural frequency. Since, in most cases, labyrinth seals are not located at shaft vibration nodes, they potentially have a more significant impact than bearings or bearing dampers on the dynamic characteristics of compressors. The vibration amplitudes at the rotor midspan are at least two to four times as large as the bearing location, depending on the stiffness ratio between the shaft and bearing. On the other hand, a damper seal or damper bearing acting directly at the center of the rotor would be most efficient in improving the rotordynamic stability of rotor-bearing systems (Lund, 1974).

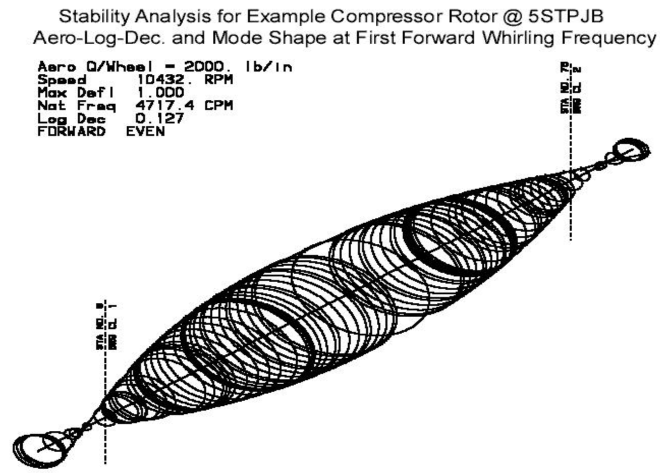

Figure 2. Rotor Mode Shape at Whirling Frequency.

Since the early 1980s, numerous investigations have been carried out to improve the dynamic performance of labyrinth seals. It seems difficult to increase the seal direct damping without changing the basic configurations of the labyrinth seals. Experiments and analyses have demonstrated that retarding the circumferential flow in the seal is a direct and effective means to reduce the cross-coupled stiffness of the labyrinth seals. The shunt injection technology has been successfully utilized to eliminate subsynchronous vibration in industrial compressors (Zhou, 1986). High-pressure gas is injected into the leading portion of the labyrinth seal in the radial direction or with an angle against the rotation direction. The circumferential swirl flow in the seal is broken up, and even the flow direction is changed in the seal by the injected gas. The authors' company has implemented this technique in their high-pressure compressors to enhance the rotor stability. However, the shunt line from the discharge volute to the seal front section should be designed and installed carefully to assure the pressure drop across the shunt line is minimized, especially for dirty working gas applications and abradable labyrinth seals using soft materials.

As early as in 1980, Benckert and Wachter (1980) verified that installing swirl brakes at the labyrinth entrance was a very useful approach to dramatically reduce the seal cross-coupled stiffness measured in their tests. The swirl brake used in their conceptual study was of simple straight shape and no geometry data of the swirl brake were provided in the paper. Later, the effectiveness of the swirl-brake technology was further demonstrated through fully instrumental experiments on TOR labyrinth seals by Childs and Ramsey (1991). However, there are few publications dedicated to the applications and experiences of swirl brakes in industrial turbines and compressors. Zeidan, et al. (1993) reported a compressor subsynchronous vibration case in which replacing the labyrinth seal with a damper seal was finally resorted to since installing swirl brakes alone could not reduce the vibration down to an acceptable level. A drop in the rotor natural frequency was observed in some experiments when the swirl brakes were used in compressors (Baumann, 1999). Recently, some CFD effort was initiated to help fully understand the mechanism of swirl brakes and optimize the design of swirl brakes (Nielsen, et al., 2001). It seems that a conventional swirl brake only adds a limited amount of seal effective damping to the rotor/bearing/seal system. Most times the conventional swirl brakes are still used as an ancillary device to back up the shunt system for high-performance compressors in the authors' company. More experimental evaluations are needed to improve the designs of the swirl brakes for more reliable antiswirl devices associated with higher seal effective damping.

POTENTIAL IMPACT OF API STABILITY CRITERIA ON THE ROTORDYNAMIC ANALYSES FOR INTERMEDIATE-PRESSURE COMPRESSORS

Six previous design cases of intermediate-pressure compressors are chosen to be reexamined per the stability screening criteria recommended by API. Actually, the related compressors have been delivered and are operating successfully with or without a deswirl mechanism. In this paper these compressors are referred to as cases A through F, respectively. Kirk and Donald (1983) proposed an empirical stability criterion using the product of the discharge pressure with the differential pressure across the compressor versus the rotor flex-ratio (operating speed to the first rigid bearing critical speed). As shown in Figure 3, the design points in Kirk's stability map for the cases A to F indicate that these compressor designs are acceptable.

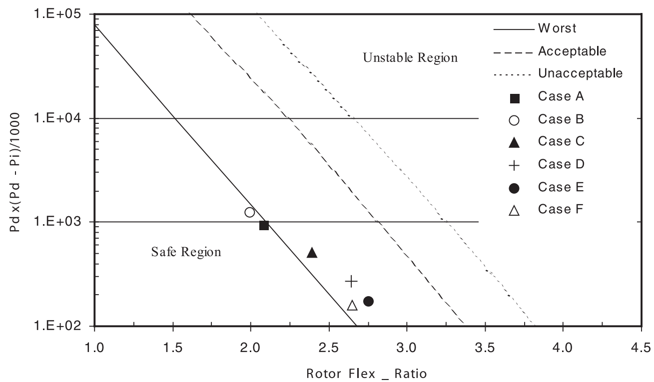

Figure 3. Compressor Design Points in Kirk's Stability Map.

All the six compressors are supported by 5 inch tilt-pad journal bearings and fitted with dry gas seals. Their average gas densities are close, varied from 1.05 lbm/ft^3 to 1.64 lbm/ft^3. Case A is a nine-stage back-to-back compressor with a maximum operation speed of 12,054 rpm and a discharge pressure of 1042 psia. In case B the compressor has eight stages, back-to-back configuration with a maximum operation speed of 12,000 rpm and a discharge pressure of 1275 psia. A radial shunt injection was designed at the center labyrinth seals in both A and B compressors to enhance the rotordynamic performance. Case C is an eight-stage flow-through compressor running at 9500 rpm with a discharge pressure of 866 psia. The balance piston labyrinth seal of this unit was shunted as well, and a conventional swirl-brake ring was used to back up the shunt system since the labyrinth teeth would run against an abradable seal stator. Case D is also a flow-through compressor with a discharge pressure of 650 psia, but its balance piston seal does not have a shunt system though this six-stage machine is running at a higher speed of 13,406 rpm. Above compressors in cases A to D were designed for natural gas services with a molecular weight from 16.2 to 18.9. Cases E and F are flow-through compressors designed for ethylene product with a molecular weight of 28.1. The unit E has six stages running at 9573 rpm with a discharge pressure of 450 psia, while the unit F has eight stages running at 10,880 rpm with a discharge pressure of 402 psia. No extra stabilizing devices, such as shunt systems and swirl-brakes, were added in both E and F compressors.

Two empirical formulas were first used to calculate the aerodynamic cross-coupling stiffness in the rotor stability analyses (aero-log-dec) for the above six compressors. The first one is the OEMs proprietary formula, which was developed at the speed and the operating conditions at which the compressors would go unstable. The predicted total cross-coupling stiffness is distributed evenly to each impeller location in the log-decrement calculation. The second one is Wachel's empirical equation based on experience from several instability problems (Wachel, 1982). The aerodynamic cross-coupling stiffness is estimated stage by stage and applied at the appropriate impeller using the Wachel formula in this paper. Both empirical formulae resulted from correlation investigations into previous centrifugal compressors that experienced rotor instability problems and have taken into account indirectly all the destabilizing effects, e.g., due to impeller eye seals, interstage seals, balance piston labyrinth seals, and oil seals, etc. The aero-log decrements are calculated at the maximum operating speeds, and the results are summarized in Table 1 for three bearing clearance cases. Note that nonsynchronous bearing coefficients are used in the stability analyses. A comparison shows that overall the predictions agree well based on both OEM and Wachel's formulae. Wachel's method results in relatively lower log-decrements for the back-to-back compressors in cases A and B. For the flow-through compressors in cases C and D, the OEMs method is more conservative with lower predicted log-decrements.

Table 1. Predicted Aero-Log-Dec per OEM and Wachel's Empirical Formulas Using Nonsynchronous Bearing Coefficients.

Case	Minimum Bearing Clearance		Average Bearing Clearance		Maximum Bearing Clearance	
	OEM	Wachel	OEM	Wachel	OEM	Wachel
A	0.060	0.005	0.154	0.094	0.276	0.203
B	0.067	0.051	0.170	0.153	0.306	0.287
C	0.058	0.088	0.134	0.145	0.170	0.174
D	0.057	0.085	0.140	0.166	0.198	0.206
E	-0.025	-0.071	0.026	-0.025	0.122	0.109
F	-0.032	-0.023	0.012	0.021	0.075	0.085

Table 2 shows the predicted aero-log decrements using the new method recommended by API (API 617, 2002). Here, Q_A is the anticipated cross-coupling stiffness that is calculated, based on a modified Wachel equation. Synchronous bearing coefficients are used, and the lumped cross-coupling Q_A and $2Q_A$ are applied at the middle impeller in the stability analyses. For level-I stability screening, acceptable criteria per API are the predicted aero-log-dec $\delta_A \geq 0.1$, with the cross-coupling Q_A at the middle impeller and the predicted aero-log-dec $\delta_{2A} \geq 0$ with the cross-coupling $2Q_A$ at the middle impeller. Examination of Table 2 finds that all the above six compressors fail to pass the level-I screening except unit D. However, unit D compressor has a flex ratio of 2.64, which is larger than the upper limit of the flex ratio for level-I stability analysis. Finally, a full rotor stability analysis (level-II) should be performed for all compressors discussed in this paper. Clearly, the rotordynamic force coefficients of major labyrinth seals have to be calculated accurately if a level-II stability analysis is required. Note that the values of the aero-log-dec in Tables 1 and 2 are not comparable directly because these aero-log decrements are calculated using different bearing coefficients, synchronous and nonsynchronous bearing coefficients, respectively. A discussion regarding level-II stability analysis per API is beyond the study scope of this paper.

TEST APPARATUS, SEAL, AND SWIRL-REVERSE RINGS

Test Rig

A cross-section of the gas labyrinth seal test stand is shown in Figure 4 without the central gas inlet chamber. This test rig was

Table 2. Predicted Aero-Log-Dec per Modified Wachel Formula (Recommended by API) with Cross-Coupling Lumped at Middle Impeller and Using Synchronous Bearing Coefficients.

Case	Minimum Bearing Clearance		Average Bearing Clearance		Maximum Bearing Clearance	
	Q_A	2 x Q_A	Q_A	2 x Q_A	Q_A	2 x Q_A
A	-0.091	-0.293	0.131	-0.103	0.322	0.052
B	-0.029	-0.169	0.218	0.053	0.446	0.252
C	0.096	-0.085	0.201	-0.006	0.317	0.155
D	0.128	0.020	0.270	0.147	0.568	0.495
E	-0.113	-0.369	0.082	-0.203	0.170	-0.143
F	-0.174	-0.399	-0.057	-0.300	0.055	-0.207

first built for gas damper seal investigations (Li, et al., 2000). Some modifications have been made since then to improve the rig hardware and instrument system for seal backpressure control and gas swirl velocity measurement at multilocations. A 50 hp variable-speed motor can drive the test rotor up to the maximum operating speed of 12,000 rpm. The main shaft diameter of the flexible rotor is 3.875 inches. The rotor has two rotating disks with 9.75 inch outside diameter (OD) and is supported on double-row angular contact ball bearings, which are located 44 inches apart. The outboard bearing uses a wave spring to compensate for relative thermal growths. Use of ball bearings instead of hydrodynamic bearings is to assure low damping for more accurate evaluation of labyrinth seal properties. Two identical labyrinth seals are back-to-back arranged in the horizontally split casing. Thus, axial thrust loads on the bearings are minimized with two gas leakage flows going out in opposite directions. The test rig is supplied with compressed nitrogen gas from a high-pressure tanker. During tests, the seal inlet pressure is set at a desired value through a controlled upstream valve providing gas to the central plenum chamber between the two test labyrinth seals. A specified pressure ratio (backpressure to inlet pressure) across the seal is maintained by controlling the seal backpressure with two automatically adjustable downstream valves. The total mass flow rate is measured with a calibrated upstream orifice. To investigate the influence of the labyrinth seal on the unbalance response, critical speed location, and system effective damping, eddy-current proximity probes are installed at each shaft end and midspan to measure rotor vibration in both vertical and horizontal directions.

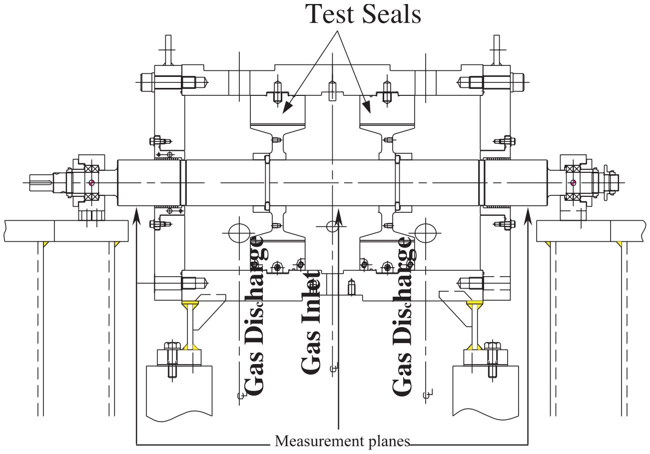

Figure 4. Cross-Section of Gas Seal Test Rig.

Figure 5 shows the gas inlet chamber and the test labyrinth seals without gas swirl-reversal rings installed. The concept of the swirl-reversal ring (vane) will be detailed later on in this paper. Spray nozzles installed on the internal inlet walls would help to generate a tangentially preswirled gas flow at the entrances of the swirl-reversal rings. The gas static and total pressures at the upstream and downstream of the swirl-reversal rings are measured. The flow direction is always positive (in the rotor rotation direction) at the vane upstream region. However, the flow direction at the vane downstream region may be in the negative or still positive direction. Between the first tooth of the labyrinth seal and the trailing edge of the swirl-reversal vane, two Kiel probes are inserted. The heads of the Kiel pressure probes point to the tangential flow direction, and their directions are against each other with 220 degrees apart circumferentially. The axial distance between the upstream and downstream Kiel pressure probes is 1.36 inches. Therefore, the effect of the swirl-reversal ring on the gas flow could be accurately evaluated by measuring the static and total gas pressures at both the upstream and downstream of the ring. When the swirl-reversal ring is not inserted, the test data of pressures can be used for estimating the influence of the pre-entrance length of the labyrinth seal on the preswirl gas flow, which is accelerated by the surfaces of the high-speed rotating disks due to the shear stress applied on the gas flow. The yaw and pitch angles of the total pressure probe are restricted within ±5 degrees with respect to the tangential direction. The pressure probes are calibrated for each test rig built-up to ensure the measurement uncertainty in the differential pressure ($P_{total} - P_{static}$) to be within ±10 percent. The upstream and downstream gas temperatures are measured as well.

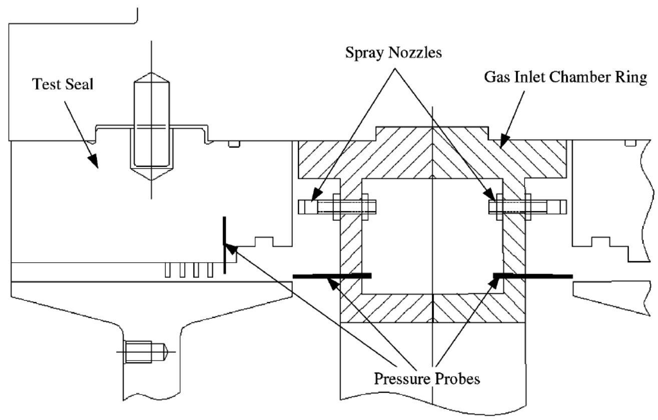

Figure 5. Central Gas Inlet Chamber Ring and Spray Nozzles.

Swirl-Reversal Rings and Test Labyrinth Seals

As we well know, a considerable amount of destabilizing forces, positive cross-coupling stiffness K_{xy}, is generated by labyrinth seals in high-performance rotating machines if the inherent preswirl gas flows are not broken down intentionally. Various shunt injections and swirl brakes have been designed and tested to retard the gas preswirl flow at the labyrinth seal entrances. Published test data and theoretical analysis results indicate that a negative or low positive preswirl flow would result in the labyrinth seals to provide rotordynamic stabilizing forces, other than inherent destabilizing forces. A new concept of antiswirl brakes was developed to further improve the rotordynamic characteristics of labyrinth seals. The new swirl-brake is referred to as swirl-reversal ring (vane) in this paper hereafter. The swirl-reversal ring can be integrated into various types of labyrinth seals through deliberated designs. Figure 6 shows simplified sketches of the swirl-reversal rings with typical straight through TOR and TOS labyrinth seals. Note that one blade is intentionally kept at the upstream of the ring. The first blade would help to form a high-velocity axial jet flow, so the downstream vane would work more effectively to turn the gas flow direction. As long as there is a leakage flow through the seal, a negative swirl gas flow is assured at the seal entrance. Clearly, the swirl-reversal ring would be more effective for TOR labyrinth seals because the whole flow path is blocked in the circumferential direction completely. For TOS labyrinth seals, some circumferentially swirled gas can still go through the gap between the rotating surface and the tip of the vane, although the main leakage flow is blocked by the swirl-reversal ring. However, limited by the existing gas seal test stand, the swirl-reversal ring was first tested with a TOS labyrinth seal without any modification on the rotating parts, and test results will be reported and discussed in this paper.

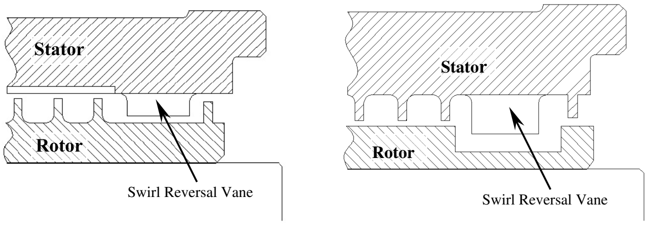

Figure 6. Swirl Reversal Vane Configurations for Labyrinth Seals.

Figure 7 shows the test TOS labyrinth seal integrated with the swirl-reversal ring inserter. The test labyrinth seal is 9.75 inches diameter by 5.25 inches long. The effective sealing length of the seal is 3.04 inches with 20 teeth matching the smooth disk surface. The test labyrinth seal has a straight-through configuration, and the nominal running radial clearance is 11 mils at 6000 rpm. The seal tooth pitch is 0.16 inches, and the tooth height is 0.18 inches. Seal tooth thickness is 0.03 inches. The gap between the vane tip and the rotating surface is 30 percent larger than the clearance at the seal teeth. The axial length of the swirl-reversal vane is 0.80 inches. Due to tests performed at different shaft speeds, a blade angle of 45 degrees is designed for the swirl-reversal vane relative to the tangential direction. In actual applications, the geometry of the swirl-reversal ring and the shape of the vane could be optimized based on machine operating conditions.

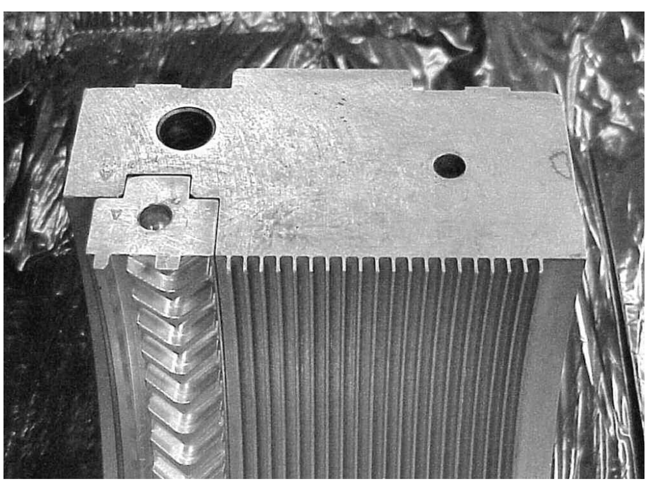

Figure 7. Test TOS Labyrinth Seal and Swirl-Reverse Ring.

EXPERIMENTAL RESULTS

Gas Swirl Velocities in Circumferential Direction

When the rotor is first brought up to 4000 rpm below the rotor first critical speed, the compressed nitrogen is added to the gas inlet chamber, and a specified supply pressure is maintained by adjusting the upstream inlet valve. The discharge valve is set up to automatically track the specified backpressure if a backpressure higher than the ambient pressure is required in the tests. The rotor is driven by the motor to pass through its first critical speed region and up to 12,000 rpm gradually while the rotor vibration is measured at the shaft midspan and both shaft ends. The gas pressure, temperature, and speed data are collected once every 2.5 seconds. The maximum supply pressure is limited to 220 psia. Based on the measured static and total pressures, gas circumferential velocities in the seal entrance region were evaluated at speeds 6000 and 12,000 rpm. In the following discussion and the figures associated, V_u and V_d are denoted as the upstream gas swirl velocity and downstream gas swirl velocity, respectively. The downstream measurement point is closer to the first tooth of the labyrinth seal.

Figures 8 and 9 show that the rotor speed is a crucial factor to determine the downstream gas swirl velocity V_d without the swirl-reversal ring installed. The trend of the swirl velocity versus the supply pressure indicates the gas swirl velocity to decrease with increasing the seal leakage rate or the gas density. The effect of the seal eccentricity (50 percent offset in the vertical direction) on gas preswirl flow is negligible. Although the gas swirl velocity is higher at the high rotating speed of 12,000 rpm, the gas swirl velocity ratio related to the rotor surface velocity is higher at the lower speed of 6000 rpm. For instance, the swirl velocity ratio is 0.45 at 6000 rpm while the ratio decreases to 0.38 at 12,000 rpm in high supply pressure tests.

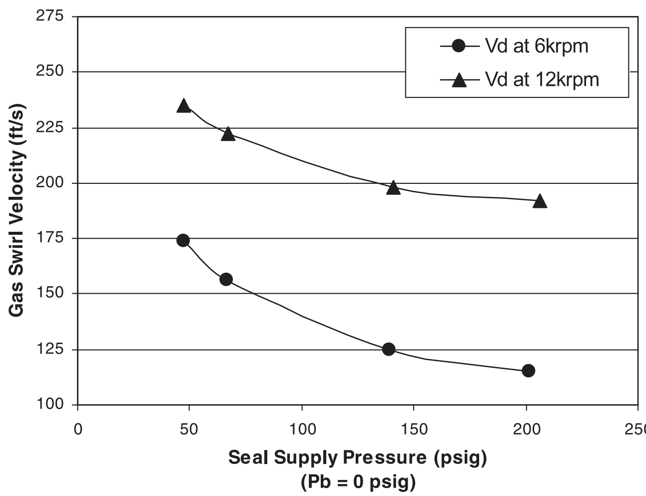

Figure 8. Measured Downstream Gas Swirl Velocity for Centered Labyrinth Seal Without Swirl-Reverse Ring.

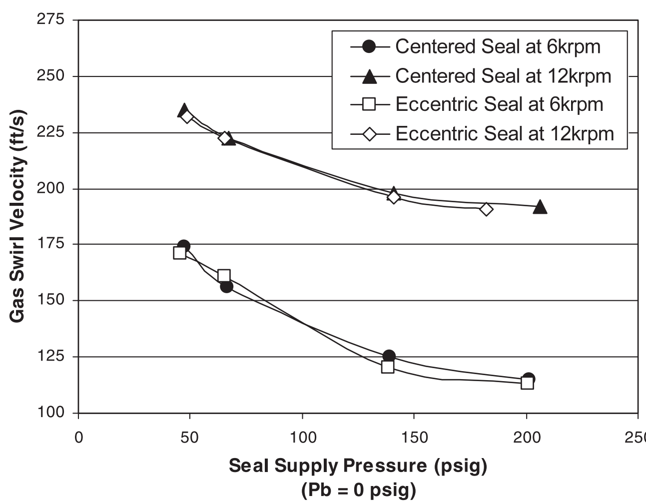

Figure 9. Effect of Seal Eccentricity on Measured Downstream Gas Swirl Velocity Without Swirl-Reverse Ring.

A comparison of the swirl velocities between the upstream and downstream flows is shown in Figure 10 for no swirl-reversal ring cases. The measurements show the gas flow has been preswirled before it enters the seal entrance region, which is about 1.5 inches long. This upstream geometric condition is somewhat similar to those applications, in which the labyrinth seals have a long pre-entrance space prior to the first tooth, or the swirl-brakes are installed at an upstream location far away from the seal. The upstream gas swirl velocity V_u remains relatively constant for three supply pressure cases. Obviously, the leakage flow is further accelerated circumferentially when the flow goes through the space encompassed by the rotating disk and the leading toothless portion of the test seal. An unexpected result is that higher gas swirl velocity ratios are measured for the lower rotor speed because the preswirled gas flow is accelerated more quickly at the low rotating speed of 6000 rpm. So far, there is no sound explanation to address the observed phenomena that the acceleration effect of the rotating disk on gas flow is minimized at the high rotor speed of 12,000 rpm. A CFD investigation has been initiated to further examine the mechanism of gas circumferential swirl in various geometric and operating conditions. Based on the experimental results, swirl brakes should be installed at an axial location as close as possible to the leading tooth of the labyrinth seal in actual applications. Otherwise the deswirled gas flow would be accelerated again by the rotating journal surface.

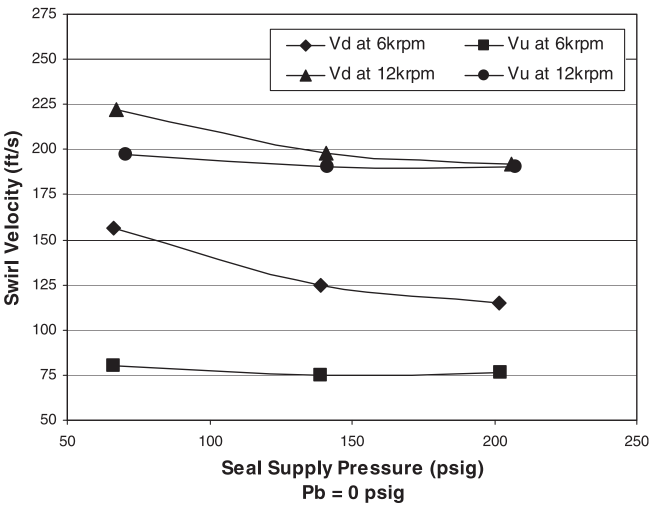

Figure 10. Effect of Long Seal Entrance on Measured Downstream Gas Swirl Velocity for Centered Labyrinth Seal Without Swirl-Reverse Ring.

Figures 11 and 12 show that the swirl-reversal ring has a strong influence on the circumferentially swirling gas flow. The downstream gas velocity is displayed in the term of $-V_d$ in these two figures, and the pressure ratio (P_b/P_s) is kept at 0.3 for all three different seal supply pressures. A positive V_u, the upstream gas swirl velocity, is always measured at the entrance of the swirl-reversal ring. However, the circumferential direction of the gas flow is completely changed when the leakage flow goes though the swirl-reversal ring for both the low and high speeds. Test results indicate that the measured downstream gas swirl velocity V_d is negative, which means the leakage flow is swirling in the opposite direction to the rotor rotation at the downstream of the swirl-reversal ring. A comparison in terms of gas swirl velocity ratio illustrates that the reversal ring is more effective at the low speed of 6000 rpm for the labyrinth seal tested. At the high supply pressures tested, the gas swirl velocity ratio is changed from a positive 0.35 to a negative 0.31 at 6000 rpm, while the gas swirl velocity ratio is changed from a positive 0.32 to a negative 0.14 at 12,000 rpm. One of the major factors to degrade the effect of the swirl-reversal ring at high speeds is that more kinetic momentum of the preswirled gas flow is carried over the gap between the rotating surface and the tip of the reversal ring for the TOS labyrinth seal tested. Contrary to the trend of the downstream gas swirl velocity V_d versus the supply pressure (leakage rate) in no swirl-reversal ring cases, the magnitude of the measured negative V_d increases slightly at the high supply pressure or high leakage rate when the swirl-reversal ring is installed. An explanation for this phenomenon is that the swirl flow has a smaller incidence angle relative to the leading edge of the swirl-reversal vanes at the high pressures tested. For the high rotating speed case at 12,000 rpm, the estimated flow incidence angle is 8 degrees at 220 psia, while the incident angle of leakage flow is 10 degrees at 70 psia, based on the measured gas swirl velocity and the gas axial velocity averaged approximately at the first throat prior to the swirl-reversal vanes. As shown in Figure 12, the effect of the eccentricity of the swirl-reversal ring on turning the gas flow is not discernable at high pressures.

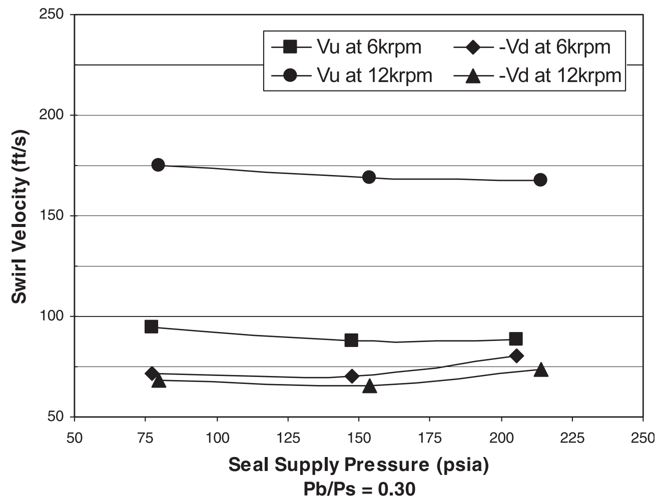

Figure 11. Effect of Swirl-Reversal Ring on Measured Gas Swirl Velocities for Centered Labyrinth Seal.

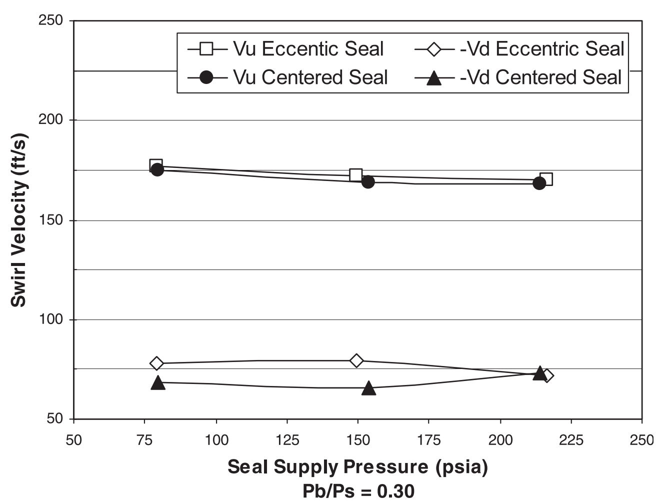

Figure 12. Effect of Seal Eccentricity on Measured Gas Swirl Velocities with Swirl-Reverse Ring at 12,000 RPM.

Results of Rotor Vibration Measurement

Examination of the rotor vibration finds that the test labyrinth seals add positive effective damping to the system to attenuate the rotor unbalance response under the experimental conditions. In most cases the maximum amplitude of the rotor unbalance response decreases consistently with the seal supply pressure. Compared to the baseline vibration characteristics of the flexible rotor tested, the critical speed of the rotor drops slightly (< 3 percent) in the test pressure ranges. At the high supply pressure of 220 psia, the observed amplitudes of the rotor synchronous vibration at its critical speed are reduced by 45 to 60 percent, approximately, in the cases even without the gas swirl-reversal ring, which indicate that the effective damping of the labyrinth seal should not be ignored in rotordynamic analyses.

One of the major concerns is the effect of the labyrinth seal and swirl-reversal ring on the rotor stability at high rotating speeds. Impact tests were performed to identify the logarithmic decrement associated with the free decaying vibration of the rotor at its natural frequency when the test rotor was running at 12,000 rpm, which is well above the rotor first critical speed. Figure 13 shows a typical rotor free-decaying vibration curve, which is extracted from the rotor transient vibration signal by using a band-pass filter to eliminate the vibration component at the rotor running speed and other minor components at higher super-harmonic frequencies. However, some existing signal noises cannot be removed since they are too close to the rotor natural frequency. These noises or vibration components, right at the natural frequency and its vicinity as shown in Figure 14, were excited by the high-pressure gas flow inside the casing. Therefore, the estimated logarithmic decrements from the free-decaying vibration curves are questionable. As an alternative to illustrate the influence of the swirl-reversal ring on the damping performance of the test labyrinth seal, the effective damping coefficients of the labyrinth seal are calculated based on the measured gas preswirl velocity at the seal entrance and are given in Table 3. The comparison of the seal effective damping coefficients indicates that more seal damping would be added to the rotor system due to installing the swirl-reversal ring at the low speed of 6000 rpm. For the rotor whirling at a subsynchronous frequency, the swirl-reversal ring would convert the labyrinth seal from a destabilizing force source into a stabilizing force source.

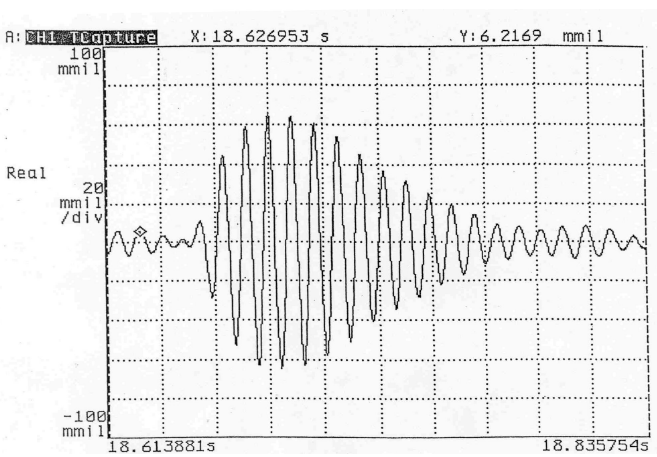

Figure 13. Free-Decaying Vibration Curve Extracted from Rotor Transient Vibration Signal.

CONCLUSIONS

● The comparison showed that the stability screening criteria per API are relatively stringent to the intermediate-pressure compressors compared to previous design and operation experience. To perform a high-level rotor stability analysis would need the OEM and customers to dedicate a considerable amount of extra effort. When the design of an intermediate-pressure compressor violates the level-I screening criteria, some existing machines similar to the new design can be used as benchmarks to help the designers and customers determine if a costly high-level stability analysis is required.

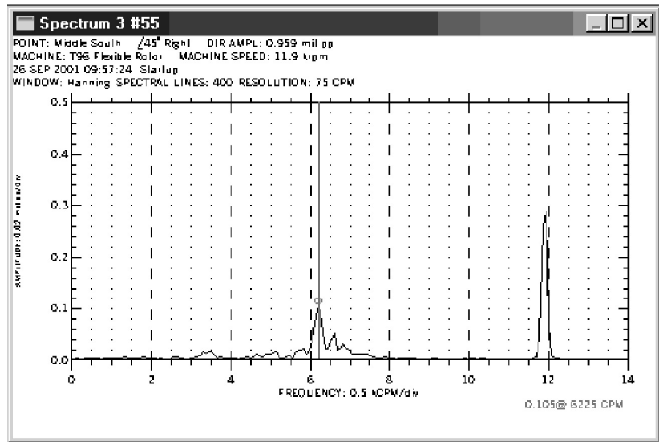

Figure 14. Background Noises (Vibration Components) in Vicinity of Rotor Critical Speed Without Impact.

Table 3. Predicted Effective Damping Coefficient C_{ef} of Labyrinth Seal Based on Measured Gas Preswirl Velocity at Pressure Ratio of 0.3.

Supply pressure (psia)	**C_{ef} at 6000 rpm for rotor synchronous whirling (lb-s/in)**		**C_{ef} at 12000 rpm for rotor subsynch. whirling at 6250 cpm (lb-s/in)**	
	No brake ring	With brake ring	No brake ring	With brake ring
70	0.4	3.3	-1.2	3.7
150	1.6	6.9	-1.6	8.0
220	2.8	10.5	-2.1	12.0

● The experimental results reported in this paper showed that the new configuration of the swirl brake is effective in reversing the circumferential swirl direction of the seal leakage flow. The swirl-reversal ring will assure a negative preswirl gas flow at the entrance of the labyrinth seal, and thereby increase the effective damping of the labyrinth seal. Using the swirl-reversal ring, the labyrinth seal will become a reliable source of stabilizing forces from a rotordynamic point of view.

● A swirl-reversal ring, when integrated into the leading portion of the labyrinth seal, would not affect any internal flow around compressor impellers.

● The measurements illustrated that the effect of the swirl brake eccentricity on the performance of the swirl-reversal ring is minor.

● The experimental data also showed that a leakage flow with a low swirl velocity will be accelerated by the rotating disk with a high surface velocity before the gas comes into the labyrinth seal. The low-density gas flow is accelerated more quickly than the high-density gas flow.

● The unbalance response measurements showed that the rotor vibration amplitude at the critical speed is attenuated by the labyrinth seal in the cases with and without the swirl-reversal ring. The damping of the labyrinth seal is not negligible in the rotordynamic analysis. The measured rotor critical speed is reduced slightly by the labyrinth seal in the test pressure range, which indicates that the test labyrinth seal has negative stiffness.

● In terms of effective damping at the rotor whirling frequency, the damping effect of the labyrinth seal on a synchronous vibration is different from that on a subsynchronous vibration. Based on the measured gas preswirl velocity, the predictions showed that the labyrinth seal has positive effective damping to suppress the rotor unbalance response while the same seal contributes a negative effective damping to promote the rotor subsynchronous vibration if the preswirl gas flow is not retarded at the seal entrance.

- It is expected that the performance of the swirl-reversal ring would become better with a higher gas swirl velocity at the upstream of the swirl-reversal ring. To achieve higher gas preswirl velocity it is planned to examine the existing gas swirl design and redesign the gas swirl nozzle system. A CFD investigation program will be dedicated to optimize the design of the swirl-reversal ring and further explore the mechanism of gas circumferential swirl in various geometric and operating conditions.

REFERENCES

API Standard 617, 2002, "Axial and Centrifugal Compressors and Expander-Compressors for Petroleum, Chemical and Gas Industry Services," Seventh Edition, American Petroleum Institute, Washington, D.C.

Baumann, U., 1999, "Rotordynamic Stability Tests on High-Pressure Radial Compressors," *Proceedings of Twenty-Eighth Turbomachinery Symposium*, Turbomachinery Laboratory, Texas A&M University, College Station, Texas, pp. 115-122.

Benckert, H. and Wachter, J., 1980, "Flow Induced Spring Coefficients of Labyrinth Seals for Application in Rotordynamics," NASA CP-2133, Proceedings of a Workshop on Rotordynamic Instability Problems in High-Performance Turbomachinery, Texas A&M University, College Station, Texas, pp. 189-212.

Childs, D. W., 1993, *Turbomachinery Rotordynamics*, New York, New York: John Wiley & Sons, pp. 290-354.

Childs, D. W. and Ramsey, C., 1991, "Seal-Rotordynamic-Coefficient Test Results for a Model SSME ATD-HPFTP Turbine Interstage Seal With and Without a Swirl Brake," ASME *Journal of Tribology*, *113*, pp. 198-203.

Childs, D. W. and Scharrer, J. K., 1986, "Experimental Rotordynamic Coefficient Results for Teeth-on-Rotor and Teeth-on-Stator Labyrinth Gas Seals," ASME *Journal of Engineering for Gas Turbines and Power*, *108*, pp. 599-604.

Childs, D. W. and Scharrer, J. K., 1988, "Theory Versus Experiment for the Rotordynamic Coefficient of Labyrinth Gas Seals: Part II—A Comparison to Experiment," ASME *Journal of Vibration, Acoustic, Stress, and Reliability in Design*, *110*, pp. 281-287.

Doyle, H., 1980, "Field Experience with Rotordynamic Instability in High-Performance Turbomachinery," NASA CP-2133, Proceedings of a Workshop on Rotordynamic Instability Problems in High-Performance Turbomachinery, Texas A&M University, College Station, Texas, pp. 3-14.

Greathead, S. and Bostow, P., 1976, "Investigations into Load Dependent Vibrations of the High Pressure Rotor on Large Turbo-Generators," *Proceedings of the First International Conference on Vibrations in Rotating Machinery* (ImechE), Cambridge, England, pp. 279-286.

Kirk, R. G. and Donald, G. H., 1983, "Design Criteria for Improved Stability of Centrifugal Compressors," Rotor Dynamical Instability, ASME, AMD 55, pp. 59-71.

Li, J., Kushner, F., and De Choudhury, P., 2000, "Gas Damper Seal Test Results, Theoretical Correlation, and Applications in Design of High-Pressure Compressors," *Proceedings of Twenty-Ninth Turbomachinery Symposium*, Turbomachinery Laboratory, Texas A&M University, College Station, Texas, pp. 55-64.

Lund, J. W., 1974, "Stability and Damped Critical Speeds of a Flexible Rotor in Fluid Film Bearings," ASME *Journal of Engineering for Industry*, *96*, pp. 509-517.

Nielsen, K. K., Childs, D. W., and Myllerup, C. M., 2001, "Experimental and Theoretical Comparison of Two Swirl Brake Designs," *ASME Journal of Turbomachinery*, *123*, pp. 353-358.

Wachel, J. C., 1982, "Rotordynamic Instability Field Problems," NASA CP-2250, Proceedings of a Workshop on Rotordynamic Instability Problems in High-Performance Turbomachinery, Texas A&M University, College Station, Texas, pp. 1-19.

Zeidan, F. Y., Perez, R. X., and Stephenson, E. M., 1993, "The Use of Honeycomb Seals in Stabilizing Two Centrifugal Compressors," *Proceedings of Twenty-Second Turbomachinery Symposium*, Turbomachinery Laboratory, Texas A&M University, College Station, Texas, pp. 3-15.

Zhou, R. M., 1986, "Instability of Multistage Compressor K1501," NASA CP-2443, Proceedings of Workshop on Rotordynamic Instability Problems in High-Performance Turbomachinery, Texas A&M University, College Station, Texas, pp. 63-75.

ACKNOWLEDGEMENT

The authors are indebted to the Elliott Company for permission to publish this paper, and to the many individuals within the company whose support and assistance made this paper possible.